

# Chapter 9

## Magnetic Pulse Compaction



### 9.1 Principles of MPC

Magnetic pulse compaction (MPC) belongs to a class of compaction methods, in which the mechanical load is applied in a (quasi) dynamic manner [1]. Along with magnetic pulse compaction, this class of compaction methods includes forging and explosive compaction. A distinctive feature of these methods is the concentration of high energy in a small volume. MPC is suitable for producing dense and porous compacts. In a non-densified state, all powders have a very poor electrical conductivity. Although magnetic field can induce eddy currents in each powder particle, they are confined in the particle itself due to an extremely high inter-particle resistance. The particles experience constriction; however, there is no mutual displacement of the particles, i.e., there is no densification. This is the reason why direct pressing of powders is not possible in many cases by applying a magnetic field to a sample composed of loose particles. In order to efficiently convert the energy of the magnetic field into the mechanical energy and gain the required pressures of the powder sample, shells made of a conductive metal (copper, aluminum) are used as containers shaping the compact and transferring pressure to the powder on a macro-level. Electrically conductive plates can also be used to transfer pressures in a uniaxial mode.

The first experiments on powder compaction using a pulse magnetic field were conducted by Sandstrom in 1964 [2]. The powder in a tube was compressed by a pulse magnetic field produced by an eigencurrent (Z-pinch schematics). The compaction occurs due to the action of the repulsive forces between the electric currents passing in the opposite directions in the coaxial conducting tubes (electrodynamics pressing). In this geometry, the shell is compressed and the powder that it contains is compacted. If the central electrode is placed inside a conducting tube, the latter can be forced to expand and thus transfer pressure in the radial direction to a tube-shaped compact [1]. Electrodynamics MPC setups were not capable of achieving high densities of the compacts due to high inductances of the current leads and other parts of the setup compared to the working elements.

Induction MPC is based on the interaction of the pulsed magnetic field with the magnetic field of eddy currents induced in an electrically conductive element – a cylindrical shell in radial compaction and a plate in uniaxial compaction. In uniaxial compaction, the principle of magnetic hammer is realized. A plate made of a conductive material is repelled from a flat inductor when a pulse of high current passes through the latter. The concentrator transfers the mechanical force to a punch, which densifies the powder in a die. This method is used to make washers and parts of complex shapes but limited heights. Barbarovich [3] applied the pulse theory to determine the velocity of the moving plate taking into account the experimentally observed facts that the motion of a part under the action of a pulsed magnetic field does not begin at once but a certain time after the beginning of the discharge. For massive parts, this usually occurs after the first current maximum, the time being needed for the energy to build up. The lower is the weight of the plate, the higher is the velocity that it develops. In radial compaction, magnetic field compresses a copper or an aluminum tube (shell) containing the powder to be compacted. The compression of the shell occurs when it is placed in a cylindrical inductor ( $\Theta$ -pinch method) or when a pulse of current passes directly through the shell (Z-pinch method). In the  $\Theta$ -pinch method, the magnetic field of the inductor interacts with the eddy currents induced in the conductive shell.

When a cylindrical electrically conducting shell is radially compressed, in the gap between the working winding of the inductor and the surface of the shell, a strong magnetic field appears for a short period of time. Due to the pulse nature of the process and a skin effect, the field does not penetrate inside the conductive shell. The outer lateral surface of the cylindrical shell experiences pressure equal to the volume density of the magnetic field [4]:

$$p = W_m = \frac{1}{2} \mu_0 \mu_r H^2, \quad (9.1)$$

where  $\mu_r$  is the relative magnetic permeability.

The resultant pressure on the powder compact is equal to the difference between the pressures on the outer and inner surfaces of the shell:

$$p = W_m = \frac{1}{2} \mu_0 \mu_r (H_1^2 - H_2^2), \quad (9.2)$$

where  $H_1$  is the magnetic field strength in the gap between the shell and the inductor and  $H_2$  is the magnetic field strength at the inner surface of the shell. The value of the pressure counteracting the pressure on the outer surface of the shell depends on the frequency of the current, the rate of change of the magnetic flux, and the electrical conductivity of the shell material. At high current frequencies, a reduction in the magnetic field strength in the direction from the surface to the interior of the conducting material can be rather significant. The electrical conductivity of the shell affects the penetration depth of the magnetic field into the shell. The penetration of the magnetic field to the inner surface of the shell would weaken the result of compression. The penetration depth of the magnetic field can be calculated as follows:

$$\delta = \frac{1}{\sqrt{\pi f \mu \sigma}}, \quad (9.3)$$

where  $f$  is the frequency,  $\mu$  is the material magnetic permeability, and  $\sigma$  is the material electrical conductivity. The thickness of the shell should be equal to or greater than the field penetration depth. When a copper shell is compressed using a  $10^4$  Hz frequency current in the inductor, the field penetration depth  $\delta$  is 0.7 mm. For the thickness of the shell equal to the field penetration depth, the field strength decreases to 37% of its initial value. When the shell is three times thicker than the penetration depth, the field strength at the inner wall of the shell is only 5%. The maximum density of the compacts is obtained when the shell thickness is close to the field penetration depth. The deformation of thicker shells causes higher energy losses and less energy is spent for the compaction process itself. However, shells that are too thin are prone to failure during MPC. After MPC, the shell has to be removed by cutting and unfolding or chemical dissolution. If reuse of the shell is possible by a certain technical approach, the manufacturing costs can be dramatically reduced.

When the skin effect is significant, the pressure can be estimated as

$$p(t) = \frac{1}{2\mu_0\mu_a} B_0^2 e^{-2\alpha t} \sin^2 \omega t, \quad (9.4)$$

where  $B_0$  is the amplitude of the magnetic induction and  $\alpha$  is the attenuation coefficient.

The electrical conductivity of the shell significantly influences the magnetic pressure. The higher is the electrical conductivity of the shell, the higher is the induced current, and, as a consequence, the higher are the magnetic induction and magnetic pressure.

In order to assess the kinetic characteristics of the MPC process based on the use of cylindrical shells, the displacement of the shell should be analyzed under the action of a pulse magnetic pressure. The equation of motion of an elementary element of the shell of external radius  $r_c$  and wall thickness  $\delta_0$  ( $\delta_0 \ll r_c$ ) can be written in the following form:

$$\rho \frac{d^2 u}{dt^2} = F_{vm} - F_{vd}, \quad (9.5)$$

where  $\rho$  is the density of the material of the shell,  $u$  is the distance,  $F_{vm}$  is the volume density of the force induced by the magnetic field, and  $F_{vd}$  is the volume density of the counter force (shell resistance to deformation). If the penetration of the magnetic field to the inner surface of the shell can be neglected, we obtain

$$\rho \delta \frac{d^2 u}{dt^2} = p(t) - p_{vd}, \quad (9.6)$$

where  $p_{vd}$  is the counter pressure, which is constant for an ideal ductile material and depends on the deformation for real materials (rapidly increases and then remains

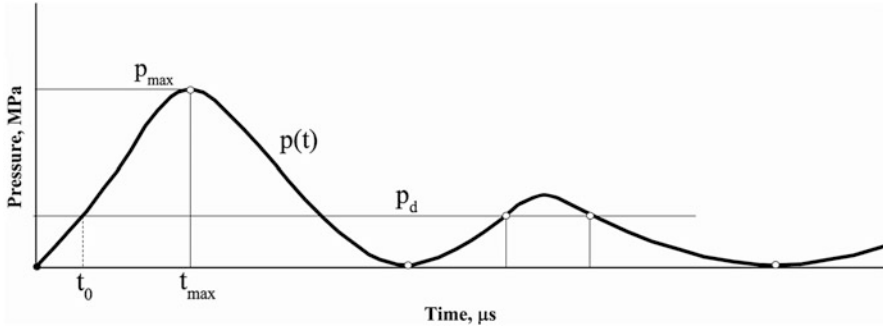


**Fig. 9.1** Evolution of magnetic pressure  $p(t)$  with time at  $p_d = \text{const}$ . (Drawn using data of Ref. [1])

practically constant as the deformation increases for cold-worked metals and gradually increases for annealed metals). Figure 9.1 shows the evolution of the magnetic pressure  $p(t)$  with time at  $p_d = \text{const}$  [1].

Due to high displacement rates of the shell and powder particles, inertia forces play a significant role. Adiabatic compression of a material induces a number of thermal effects in the compact. The heat is also transferred from the shell carrying the eddy currents. The presence of pores in the material that is to be compressed in the MPC is responsible for an increase in the fraction of the thermal energy dissipated into the material, which is related to local deformation and adiabatic compression of air filling the compressed pores.

In MPC, the pressure increases more slowly than in explosive compaction, which is characterized by a rapid pressure increase during a short pulse of 1–10  $\mu\text{s}$ . In MPC, the pulse duration can be varied by adjusting the experimental parameters. This eliminates the unloading wave which could otherwise have followed the compression wave and prevents crack formation in the compacted materials. The pulse duration in MPC ranges usually from tens to hundreds of  $\mu\text{s}$ . Unlike the dynamic pressing, MPC generates an acclivous leading edge of the compression wave, which excludes the emergence of the next discharge wave and avoids exfoliation of the compacts.

## 9.2 Equipment for MPC

At present, the MPC method uses two technological schemes, which are based on uniaxial and radial compaction. Figure 9.2 shows a magnetic pulse press for flat uniaxial compression. As the magnetic field in the plate is completely damped, an analogy may be drawn between the electromagnetic forces acting on an electrically conducting surface and a gas exerting a pressure on it.

The main requirements for conducting a successful MPC process are a high electrical conductivity of the shell, a short distance between the inductor and the accelerated part, a high energy of the magnetic field, and a high rate of change of the magnetic flux.

**Fig. 9.2** Magnetic pulse press for flat uniaxial compression: 1, inductor; 2, metallic plate (concentrator); 3, punch; 4, die; 5, powder; 6, base. (Drawn using data of Refs. [5, 6])

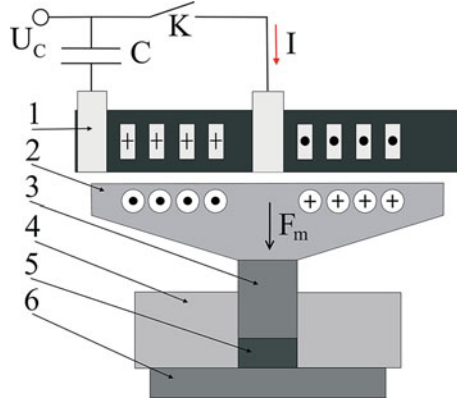


**Fig. 9.3** An assembly for radial MPC [7]: 1, copper shell; 2, rod; 3, powder; 4, bushing; 5, gasket; 6, plug. (Drawn using data of Ref. [7])

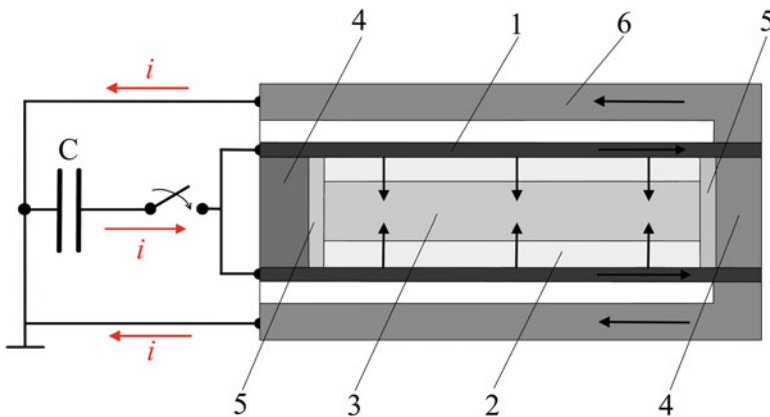
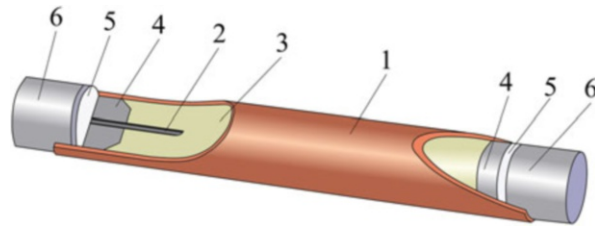


**Fig. 9.4** Principle scheme of magnetic pulse compaction of tubes: 1, copper shells; 2, powder; 3, steel rod; 4, plugs; 5, gaskets; 6, reverse conductor. (Reprinted from Ivanov et al. [8] [http://www.iiss.sanu.ac.rs/download/vol37\\_1/vol37\\_1\\_06.pdf](http://www.iiss.sanu.ac.rs/download/vol37_1/vol37_1_06.pdf), this article is available under the terms of the Creative Commons Attribution License (CC BY), <https://creativecommons.org/licenses/by/4.0/>)

The radial MPC (Fig. 9.3) is suitable for making tubes and rods several tens of centimeters long. Figure 9.4 is suitable for both  $\Theta$ -pinch and Z-pinching schemes.

The technology of MPC is promising for consolidating long-length parts. For ductile materials, MPC allows obtaining nearly fully dense compacts without a

heating stage. Powders of materials that lack ductility can be compacted by MPC to densities exceeding 0.8 of theoretical density, while full densification can be achieved by the subsequent sintering. Due to a strained state of the material and high concentrations of defects in the particles, the required sintering temperatures are reduced such that a nanostructure of the material can be preserved in the sintered state. Both conductive and non-conductive materials can be compacted. The magnetic pulse compaction approaches have been successfully used for the pressure treatment of nanosized powders [7–10].

The powder compaction involves several distinct stages [11]: 1) packing (particle rearrangement), 2) elastic deformation at contact points and 3) plastic deformation at contact points of ductile particles and fragmentation of brittle ones. In the powder just loaded into a shell or a die, groups of particles become locked by friction. As the punch moves down toward the powders, the particles move to lower positions until further movement is not possible without particle deformation. At the end of the first stage, the particles form a rigid system. During the second stage, sliding between the particles and elastic compression at the contact points result in further densification of the powder. During the final stage, the material around contact points is subject to plastic deformation and flow. At this stage of compaction, there is a significant increase in resistance to densification due to strain hardening (cold working). Figure 9.5 demonstrates that multiple impacts are more effective as long as no delamination effects appear [11], which agrees well with Ref. [12].

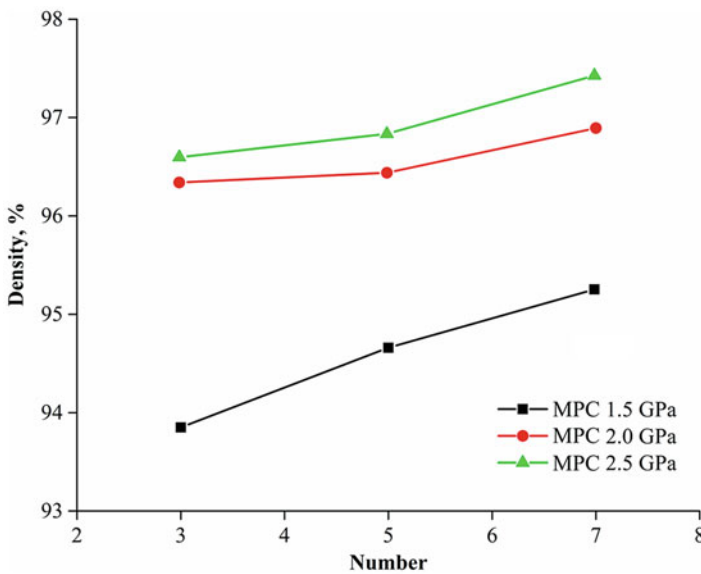


**Fig. 9.5** The density of compacts after multiple pressing cycles. (Reprinted from Park et al. [11], Copyright (2012) with permission from Elsevier)

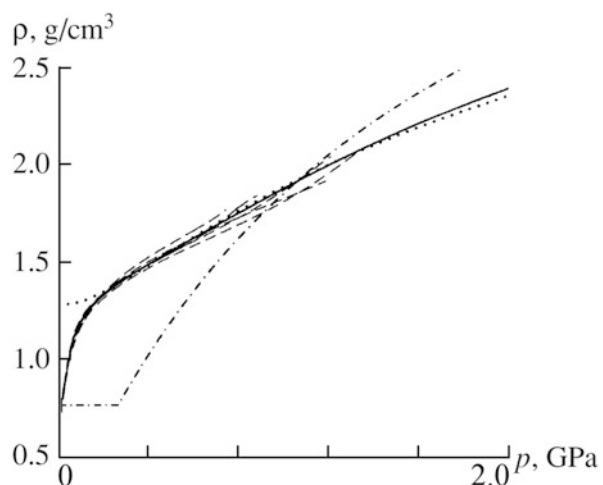
### 9.3 Modeling of Uniaxial and Radial MPC

Despite a rather long history of the experimental research, the systematic theoretical description of MPC started only in the 2000s. Reference [13] describes the first attempt of the modeling of the radial compression of a powder, taking into account the dynamic effects that appear when the can is accelerated by an external pulse magnetic field. The so-called inertia effect is noted in this work, when due to the inertia of the mechanical system (the can and the powder), a pressure level can be achieved that is significantly higher than the stress applied to the can by the magnetic field. It should be noted that the dynamics of the electric circuit has not been considered (the magnetic field pulse was defined by a decaying sinusoid).

The theoretical description of uniaxial pressing was developed by Boltachev et al. [14, 15] by assuming that the punch (impactor) acceleration by the magnetic field and the pressing of a powder occur independently; i.e., first, the acceleration of the impactor (which is not in direct contact with the powder) occurs, and after that the impactor comes into contact with the powder, and the powder compression occurs.

A theoretical model for radial MPC was developed by Boltachev et al. [9, 16], who found a closed solution of both the equations of the dynamics of a mechanical deformed system (a powder and a shell) and the equations of the dynamics of an electric circuit, which generates the magnetic field. By simultaneously solving the differential equations, it is possible to bring the theoretical models to the level of exact quantitative predictions and fully characterize the process. The powder compaction was described within a continual approach of plastically hardened porous body using empirical laws of hardening, in which the free parameters were determined from the experimentally obtained adiabatic curves of uniaxial compaction, examples of which are shown in Fig. 9.6 [17].

**Fig. 9.6** Adiabatic compression curves for an alumina-based nanopowder produced by electric explosion: dash-dotted line is a theoretical case with the constant yield stress of 2 GPa, dotted line is the theory with a parabolic hardening law, solid line is the case with a modified hardening function, and dashed lines are experimental curves. (Reprinted from Boltachev et al. [17], Copyright (2007) with permission of Springer)



The theoretical modeling demonstrated that a satisfactory description of the radial compaction of powder in accordance with the Z-pinch mode can be achieved based on the approximation of a pronounced skin effect. At the same time, the simulation of the densification processes in the  $\Theta$ -pinch mode requires the consideration of the diffusion of the magnetic field in the conductive material (shell, solenoid) and of their heating, largely due to the passage of electric current.

The complete system of equations, which takes into account all these factors in relation to the movement of a hollow shell, was formulated in Ref. [18]. It should be noted that for a fixed shell and neglecting heating of the material, the problem of the diffusion of the magnetic field is described by a linear differential equation, and its solution is possible in a closed form [19, 20]. Such an analysis, in particular, enables the determination of the scope of the problem parameters (size of the shell, the amplitude, and pulse width of the external magnetic field), when the shell's volume can be expanded by the residual magnetic field present in its cavity. This effect is seen as a possible way of a noncontact removal of spent shells from the compressed products. Developed in Ref. [18], the theoretical model was generalized in Ref. [16] to describe the motion of a shell in the presence of a densifying powder inside it. The analysis of pulsed processes of radial compaction based on the simultaneous solution of differential equations defining the dynamics of the electric circuit and the system being deformed, was carried out. This allowed studying the influence of various experimental setup parameters on the compaction process. Inertia effects in compaction dynamics were investigated, and the "resonance" compaction conditions, corresponding to the maximal usage of the inertial properties of the "powder + shell" system being deformed, were revealed. Thus, a theory of powder pressing for the  $\Theta$ -pinch mode, sufficient for reliable reproduction of the known experimental data and, as a consequence, for the confident prediction of these processes, was created.

The correctness of the theoretical model was confirmed by a direct comparison of the calculated data with the existing experimental data on the nanopowder compact final density (green density). The theoretical model (taking into account the magnetic field diffusion) was developed for the pressing by relatively thin-walled conducting shells with a thickness that is comparable to or less than the magnetic field skin layer characteristic thickness. In particular, within the model, the cylindrical shell expansion caused by the diffusion of the magnetic field inside is studied. This effect was experimentally confirmed and is considered as one of the options of the shell detachment from the compact [16]. In general, the developed theoretical models allow performing a reliable prediction of the processes of nanopowder MPC and choosing the optimal conditions for manufacturing compacts with the required characteristics. It has been shown that the theory of plastically hardened porous body allows us to correctly characterize the nanopowder compaction process at a macroscopic level. Tuning of the resonant conditions is possible by varying both the external action characteristics (electric circuit parameters) and the inertia properties of the mechanic system being deformed. Within the  $\Theta$ -pinch theory taking into account the magnetic field diffusion, complete agreement is achieved between the theoretical calculations and the experimental data on powder compact final densities.



Mathematical models have not only enabled determining the features of the compaction processes, but also helped discover a phenomenon of the shell expansion at the end of the pulse previously not known from the experiments but very useful for the procedure of detaching the shell from the compact.

The mathematical models and calculation methods elaborated for the radial MPC were successfully transferred to a more complex object for modeling – uniaxial MPC. In Ref. [10], the size effect was considered, which is one of the most important effects for any type of the compaction processes. In that publication, the size effect was related to the size of the powder particles. Calculation performed for particles ranging from 10 to 100 nm taking into account Hertz elastic forces, tangent friction forces, and dispersion forces of attraction have shown that the latter make fine powders more difficult to densify than coarse powders.

A mathematical model of uniaxial MPC of powders that includes a consistent solution describing the dynamics of a pulse magnetic field and the dynamics of the mechanical system (the moving pressing parts + compacted powder), was presented by Olevsky et al. [21]. The model takes into account a number of important factors such as dissipative losses at the friction contact boundaries, the elastic properties of the pressing device, and the inertia properties of the moving parts of the press. The constitutive behavior of the compacted powder is described in the framework of the theory of plastic porous bodies with hardening [17, 22–27]. To determine the number of parameters of the theory (the law of hardening of a powder body, the coefficients of friction, the elastic characteristics of the press, etc.), experimental research on pressing of two different nanosized powders of alumina has been conducted. It was shown that the developed theoretical model can reliably reproduce the results of the conducted experiments: the time cyclograms of the electric current passing through the inductor and of the force (pressure) applied to the compacted powder can be described with the accuracy comparable to the scale of the experimental measurement error. For a known pressure applied to the powder, and for the established laws of hardening, the theory allows estimating the evolving density (and/or porosity) of the powder specimen and, consequently, selecting the optimal pressing conditions enabling the achievement of a desirable level of final porosity. The developed theoretical model allows analyzing a variety of pressing conditions, without making expensive, and sometimes unrealizable with the existing equipment, experimental studies. Although a decrease in the powder mass can slightly increase the final density of powder compacts, more promising would be the downsizing of the accelerated components of the pressing device (Fig. 9.7).

Rather high requirements to the strength characteristics of the impactor prevent such a tangible reduction in its mass. Increasing the diameter of the powder specimen needed during the transition from test lab-scale experiments to the fabrication of practically significant components, for fixed energy costs, of course, reduces the final density. The developed theoretical model enables the prediction of the results of compaction in the dies with different diameters. In particular, for dies with diameters of up to 35 mm, calculations show that a proportional increase in the charging voltage and the diameter of the die does not change the final porosity of the powder specimen. However, note that, in general, the presence of the dissipative terms in the

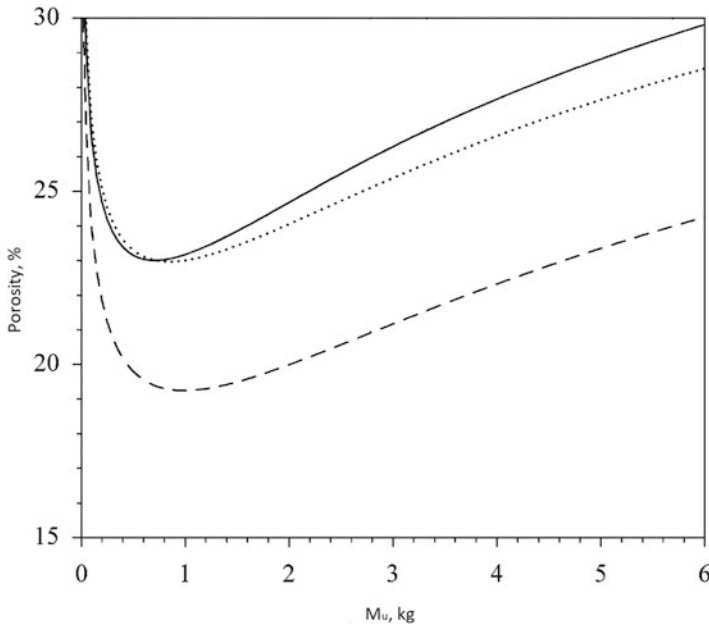


**Fig. 9.7** Porosity  $\theta$  of the compacted alumina as a function of the impactor mass  $M_u$  (solid line,  $m_p=1.5$  g (powder mass),  $U_0=2.0$  kV; dashed line,  $m_p=1.5$  g,  $U_0=2.5$  kV; dotted line,  $m_p=1.0$  g,  $U_0=2.0$  kV. (Reprinted from Olevsky et al. [21], Copyright (2013) with permission of Springer)

constitutive equations of the model violates this simple way to scale. The ways to significantly increase the final density of a powder compact at a given charging voltage of the capacitive storage are particularly relevant for large-diameter compacted products. One approach consists in varying the natural period of the electric circuit. When the electric current increases the time in a circuit equal to (approximately) the time of the realization of the pressing process (time before the stop of the impactor), there is a kind of resonance – the force exerted by the impactor on the powder specimen can substantially exceed the amplitude of the magnetic field impact on the impactor. This effect is achieved through the best use of the inertia properties of the impactor.

Double-sided MPC was studied by Barbarovich [3] as a more economical and more efficient variant of MPC. In search of methods of enhancing the efficiency of MPC, double-sided MPC has been recently revisited [28]. Double-sided MPC allows achieving higher densities of the compact relative to the single-sided scheme (Fig. 9.8, see also Fig. 9.2). The double-sided method uses two impactors, which are moving toward each other and densify the powder volume located between them (Fig. 9.8). The utilized concentrators have a serial connection. A comparison of the single- and double-sided compression schemes is shown in Fig. 9.9 for an alumina nanopowder. An increase in the total inductance in the double-sided scheme reduces the amplitude of the current in the circuit and, consequently, leads to a decrease in

**Fig. 9.8** Principle scheme of double-sided MPC:  
 1, powder; 2, die;  
 3, punches; 4, concentrators;  
 5, satellites; 6, inductors.  
 (Drawn using data of Ref. [28])

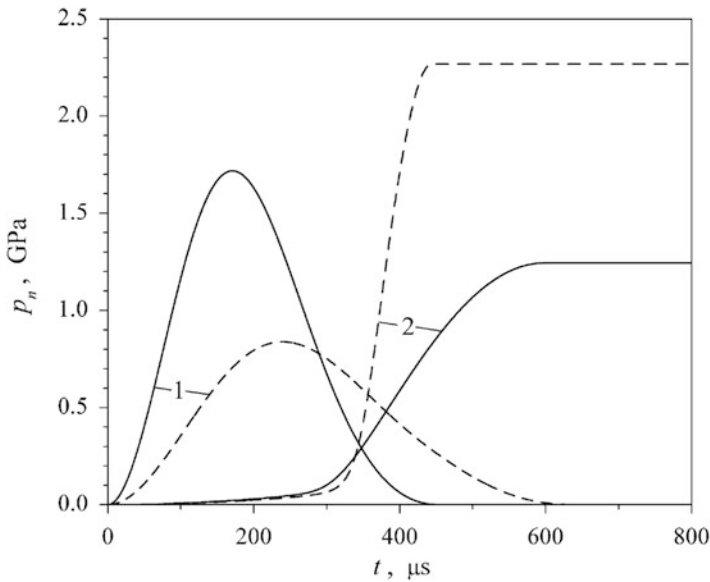
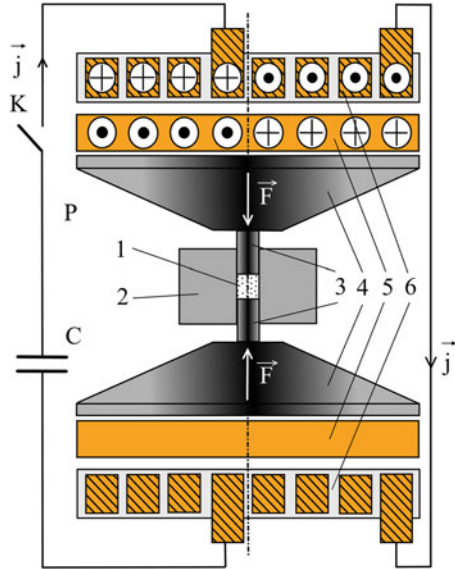


**Fig. 9.9** “Magnetic pressure” normalized with respect to the specimen’s cross-sectional area (lines 1) and pressure acting on the densified powder (lines 2). Solid lines, single-sided MPC; dashed lines, double-sided MPC. (Reprinted from Olevsky et al. [21], Copyright (2013) with permission of Springer)

the “magnetic” force acting on each of the impactors (Fig. 9.9, lines marked 1). However, the force on the powder is not reduced; on the contrary, as seen in Fig. 9.9, lines marked 2, it increases, leading to a decrease in the final porosity (from 34.8% in single-sided pressing to 29.6% in double-sided pressing). This occurs mainly because of exclusion of the effective elasticity of the pressing device from the process. In such a setup, all the momentum reaching the powder is spent on its pressing and not wasted on the elastic deformation of the lower part of the press. A positive factor is the growth of the natural period of the circuit oscillations due to an increase in its inductance. This shifts the mode of operation of the pressing device to the “resonant” pressing conditions. Note, however, that the double-sided compression method requires substantial modifications of the existing equipment for MPC.

The final goal of MPC is to fabricate parts with desired characteristics, which include geometry, porosity, density distribution, microhardness, fracture toughness, breakdown voltage, and other functional properties. In order to fabricate a part, an optimal choice of independent as well as dependent parameters should be made including the parameters of the powder (the material of the particles, composition of the powder mixture, particle size, particle shape), parameters of preliminary treatment (pre-pressing, degassing, preheating), and parameters of the pulse (the pressure amplitude in the pulse, waveform of the pulse, pulse duration, the number of pulses in a series or the law governing the series of successive pulses).

With many parameters inherent to MPC, a large number of experiments may be necessary for the process optimization. Knowledge of the process mechanisms at the pre-compaction stages as well as those during MPC makes it possible to develop an efficient fabrication technology. The problem becomes even easier to solve when the understanding level of the processes allows describing them mathematically and developing software capable of calculating the required technological parameters.

Poor densification of alumina nanopowders predicted theoretically was verified experimentally using powders having particles in the range of 21–82 nm [10]. It was found that the size effect is observed at a pulse pressure of 0.1 GPa, while at 1 GPa, the residual porosities of the compacts produced from different powders coincide within the limits of the measurement error. The authors suggest that this qualitatively distinguishes oxide powders from metallic powders, in which the size effects are observed up to pressures of several GPa. In metallic powders, the ability to deform increases with the particle size; in oxide powders, even coarse particles are mechanically strong. It is thus believed that the only reason for the size effect is the action of inter-particle dispersion forces of attraction. The authors of Ref. [10] have also modeled multi-cycle compaction, in which the powder is subjected to several pressing pulses. The calculations have shown that multi-cycle loading allows achieving densities close to the theoretical one. The efficiency of the proposed method was verified by the experiments with the Ti6Al4V alloy [12] and aluminum alloy powders [11].

Microstructure investigations of a copper compact obtained by uniaxial MPC showed that the porosity increased with the distance from the moving punch [29]. The same effect was observed in uniaxial MPC of titanium nitride [30].

In order to achieve a more uniform densification, it was proposed to conduct another pressing cycle after turning the compact in the die by  $180^\circ$  [29]. Applying two pressing cycles has given good results for an aluminum-based powder [11]. It was found that the compact density decreased as the amount of the powder in the die increased. This effect was more pronounced at low compaction pressures.

The role of preliminary pressing on the final density of the material produced by MPC was studied. Densification of an alumina powder prior to MPC resulted in a decrease in the final density of the compact [31]. However, an opposite result was described in a later publication [32]. An increase in the initial density of the powder load by static pre-pressing resulted in higher densities after MPC as no work of the external force was necessary to achieve denser packing of strong powder agglomerates, so the energy was more efficiently used for the fracturing process.

It was shown experimentally that the agglomerated state of nanopowders plays a major role in the pressing processes [32]. The presence of large and strong agglomerates makes it more challenging to compact a powder by MPC and obtain high final densities. This can be a consequence of the size effect; however, this was not taken into consideration in the modeling studies presented in Refs. [33, 34].

A certain number of aspects of MPC have not been investigated to date. Processes at the particle scale have been rather scarcely addressed. The influence of the compact size on the results of uniaxial MPC was not studied, while this was studied for radial MPC. Effects specific to compaction of shapes other than axisymmetric have not been yet investigated. The roles of pre-pressing, the presence of absorbed species, and temperature of the process have not been addressed in detail. In nanopowders, the content of absorbed species can be up to several percent, and their presence can cause the formation of cracks in the compacts. This issue was addressed in Ref. [35] for alumina and rather briefly in Ref. [36] for zirconia.

Understanding of the process mechanisms includes not only the micro- and macro-level phenomena in the powder compact but processes in the MPC tooling, such as elastic vibrations of the punches in uniaxial MPC, deformation kinetics of shells in radial MPC, and the interaction of the external magnetic field with the powder particles.

Sintering of materials compacted by MPC is not widely presented in the literature, nor is the influence of the defects and strain accumulated during MPC on their sintering behavior.

MPC offers possibilities of preserving the nanostructure of the compacted materials and making parts with a wide range of shapes – from disks and pellets to long-length rods and tubes. A significant advancement in the understanding of the processes during MPC has been made in the past decade thanks to computer modeling. The future development of the technology of MPC is thought to benefit from multiple compaction pulses, compaction in two pulses with turning of the sample before the second pulse, expansion of the shell at the end of the pulse, as well as a combination with spark plasma sintering (SPS). Using multiple pulses helps achieve high compact densities without any risk of tooling damage. The second pressing cycle applied to the sample can be helpful in reaching a uniform density in thicker samples. Process parameters favoring shell expansion would make it easy to

remove the compact from the tooling. Recent studies have shown that a possibility exists to switch from conventional sintering of MPC-produced parts to SPS. Ceramic materials obtained by this combination are fully dense and possess a nanostructure inherited from the powders.

## 9.4 Selected Examples of Application of MPC to Different Materials

The main goals of experimental MPC studies of metals are to fabricate nanostructured metals, which presumably possess improved mechanical properties important for practical applications, and gain a deeper understanding of the mechanisms of MPC of nanopowders using simple model systems. As MPC can be successful for nanopowders, fine powders with a narrow particle size distribution are the systems that draw major attention. Figure 9.10 shows that the grains in a compact produced by MPC are much finer than in a conventionally sintered compact [37].

Figure 9.11 shows the relative densities of different materials produced by MPC including soft aluminum and brittle alumina and silicon carbide.

MPC is effective in producing metallic parts from powders. The compacts exhibit properties that make them suitable for practical application without a post-compaction annealing operation. MPC is effective for both coarse powders and nanopowders. At low compaction pressures, in order to achieve full densification and desired properties, ductile metals should be compacted by a series of pulses. A higher density and a more uniform microstructure of the compact are obtained when two pulses of compaction are applied, the part being turned by  $180^\circ$  before the second pulse. It is believed that for each metal, a critical pulse pressure exists that can ensure full densification in a single-pulse compaction process. If several pulses are applied to metals that lack plasticity, fragmentation of the particles occurs, and properties of the compact affected by the inter-particle interaction forces deteriorate.

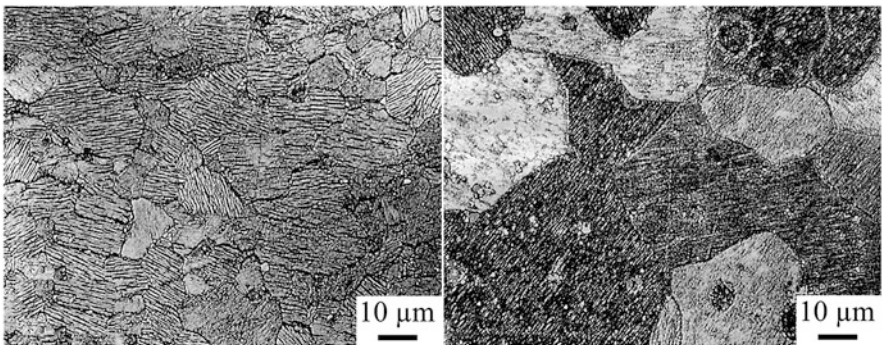


**Fig. 9.10** Microstructure of a SmCo compact produced by MPC (left) and conventional sintering (right) [37]

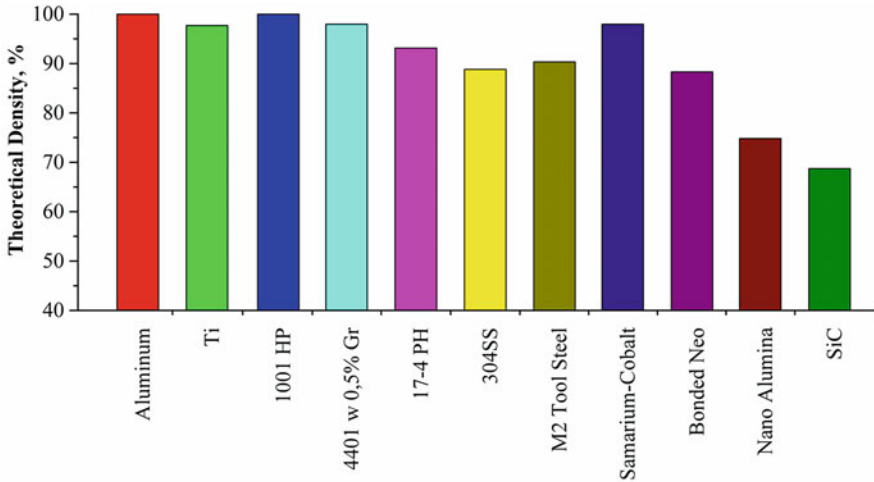


Fig. 9.11 Relative densities of materials compacted by MPC [37]

Uniaxial MPC of copper was reported in Ref. [29, 38, 39]. The following results have been obtained: uniaxial MPC of copper nanopowder at 1.5 GPa results in the formation of compacts 95% dense; the hardness of the compacts increases with the compaction temperature up to 300 °C, while their nanocrystalline structure is preserved; when the temperature increases up to 400 °C, significant grain growth occurs with simultaneous drops in density and microhardness.

The density of aluminum compacted at 1.6 GPa and 300 °C varied between 94% and 95% [40]. As the compaction temperature increased, the pore size also increased but the total volume fraction of the pores decreased. In Ref. [41], fabrication of a 97.6% dense Al compact at a pressure of 1.6 GPa and 300 °C was reported. The same evolution of pore distribution as in Ref. [40] was observed and related to fragmentation of the oxide films. Uniaxial MPC of an Al–20% Si powder with an average particle size of 106 μm at room temperature was studied [11]. The highest density (98%) was achieved when two pressing pulses were performed; the compaction results largely depending on the value of pressure applied during the second compaction cycle.

In Ref. [42], it was found that pretreatment of the powder affected the density of the iron-based compacts consolidated by MPC. The maximum density of the compact (82.1%) produced by MPC was reached when the powder was milled for 4 h (the particle size up to 50 μm) and annealed at 600 °C for 1 h. Uniaxial MPC was carried out at a pressure of 1.5 GPa. The only information on record on MPC of steels comes from publications by IAP Research (USA) [43]. Fabrication of compacts 99% dense from steel powders was reported.

Uniaxial MPC of Mg–Zn<sub>4.3</sub>Y<sub>0.7</sub> was presented in Ref. [44]. It was shown that under the maximum value of discharging voltage, the compact density was only 96%. The authors suggest that the residual porosity and poor mechanical

characteristics of the compact were due to the presence of an oxide film on the powder surface and a limited slip system in the magnesium crystalline structure. A nearly fully dense compact was obtained after compaction at 300 °C showing a 13% increase in hardness.

Nanostructured ceramic materials are attractive structural materials due to their high strength, hardness, and fracture toughness. Among consolidation methods that allow preserving the nanostructure of the powders in the consolidated material, MPC is one of the most promising. Unlike metals, ceramic particles are not capable of plastic deformation, and, therefore, MPC of ceramic materials cannot produce compacts ready for the practical use. In order to obtain fully dense materials, a post-compaction sintering step is necessary. Alumina powders are the most popular objects in the studies of dynamic compaction as these powders are inexpensive and have a broad range of applications. The uniaxial MPC of alumina nanopowders was systematically addressed in Ref. [31]. The size of the powder particles was 20 nm. The pre-pressed powder was subjected to vacuum degassing at 300 and 600 °C in a chamber up to a pressure of 1 Pa. It was found that preliminary densification of the powder leads to a decrease in the density of the MPC-produced compact. As the pulse pressure increases up to 2 GPa, the density of the compact increases. Densities ranging from 52% to 83% were obtained; the compacts did not show any inner cracks. In a continuation of this research [45], it was found that when a static pressure of 1.6 GPa is used, the optimal degassing temperature is room temperature, which indicates a positive effect of the absorbed species reducing the inter-particle friction. It was concluded that pressure in the pulse is not the only parameter affecting the compaction results.

Sintering of nanostructured alumina compacts produced by uniaxial MPC was studied in Ref. [46] as the final processing stage of the consolidated material. It was found that sintering would result in a fully dense compact, if the compacts produced by MPC were 70–80% dense, which is rather easy to achieve. Optimization of the heating regime has been performed considering the phase changes in the material. It was found that fast uncontrolled heating is not suitable for sintering of pressed parts from nanosized powders as it causes expansion of the material and results in low final densities. The result of the study was the preparation of 97% dense  $\alpha$ -Al<sub>2</sub>O<sub>3</sub> with a grain size of 100–150 nm.

A study had been carried out to compare the effectiveness of the Z-pinch and  $\Theta$ -pinch methods for pressing of two types of alumina nanopowders containing magnesia [7]. An original powder holder has been designed, in which both methods can be realized under the same conditions. The holder was designed in such a way that it was possible to conduct hot degassing and seal it before placing it in the MPC facility. Better results were obtained with the  $\Theta$ -pinch method, in which the same parameters of the generator resulted in a longer pulse. Pressing of powders having particles of 20 and 90 nm by radial MPC and by the static method showed that in all cases higher densities were obtained using non-agglomerated powders. However, compacts from agglomerated powders showed a more uniform density along the radius of the compact.



The dependence of the final density of the MPC-produced compact on the green density was studied for several alumina-based nanopowders containing different additives [47]. For experiments on radial MPC, the powders were poured into a thin-walled tube with an outer diameter of 12–14 mm and a central channel 2–3 mm in diameter. Radial MPC was performed at a pressure of 0.3 GPa and a pulse duration of about 100  $\mu\text{s}$ . A compact with a uniform microstructure was thus obtained and was 55–60% dense. In parallel experiments, powders were processed by uniaxial MPC, which resulted in the formation of a disk 15 mm in diameter and 1 mm thick with a relative density of 56–85%. The pressed compacts were sintered at temperatures up to 1550 °C for 5 h. When sintering of pure  $\alpha\text{-Al}_2\text{O}_3$  was carried out at 1550 °C, densities of the pressed compacts exceeding 2  $\text{g/cm}^3$  led to a decrease in the final sintered density. When a nanopowder of an Al–Mg alloy was added to  $\alpha\text{-Al}_2\text{O}_3$ , the final sintered density was practically independent on the density obtained at the compaction stage. For powders annealed at 1400 °C, the final sintered density increased as the density of the MPC-produced compact increased up to 2.8  $\text{g/cm}^3$ . The best mechanical properties and structural characteristics were obtained using a corundum powder containing 15% of an Al–Ag alloy. The density of the sintered material was 97%, its microhardness was 18–20 GPa, and its grain size was about 1  $\mu\text{m}$ .

References [48, 49] report the formation of 94% dense crack-free  $\alpha\text{-Al}_2\text{O}_3$  compacts after uniaxial MPC at 1.25 GPa and sintering at 1450 °C for 3 h. However, better results were produced by a combination of uniaxial MPC and SPS [50]. After uniaxial MPC at a pressure of 2.1 GPa and subsequent SPS for 10 min at 1350 °C (heating rate 100 °C/min) and a pressure of 50 MPa, bulk samples with a relative density of 99.7% were obtained. No grain growth was observed after these operations. It is interesting to note that  $\text{Al}_2\text{O}_3\text{-ZrO}_2(\text{Y}_2\text{O}_3)$  nanosized composite powders compacted by MPC up to a relative density of 55% could be sintered to a density of 99% by SPS at 1350 °C [51]. This shows that a combination of MPC and SPS is very promising for the fabrication of dense ceramics.

The behavior of  $\text{ZrO}_2$  during compaction was reported in a number of publications [52, 53]. The compaction resulted in the formation of 80% dense materials, which were further densified during sintering up to a density of 96%. Radial MPC followed by sintering at 1600 °C was used to consolidate yttria powders [54, 55]. After MPC the density was 69%; after sintering it increased to 98.6%.

The successful process of MPC depends on the plasticity of the material or the content of a binder. Therefore, composite mixtures can be anticipated to behave during MPC in a way similar to metals. The details of MPC of Al– $\text{Al}_2\text{O}_3$  were presented in Ref. [56]. The size of  $\text{Al}_2\text{O}_3$  particles was 40 nm, while the size of Al particles was 154 nm. The grain size of the sintered materials was 1–2  $\mu\text{m}$ . The best mechanical properties were observed in the composite containing 15% of Al compacted at 0.3 GPa and sintered at 1550 °C. The microhardness of the composite was 19.4 GPa, and its fracture toughness was 7.3  $\text{MPa}\cdot\text{m}^{1/2}$ .

MPC of Co–diamond composites was studied by Lee et al. [57]. After compaction at 4 GPa, the density of the material was 86.4%, and upon subsequent sintering it increased up to 99.6%. The hardness of the material was 99.8 HRB. Compared

with conventionally processed Co–diamond composites, composites produced by MPC were denser and had higher hardness and smaller grains. The compacts produced by this technique can be used in drilling tools and offer longer service lives of the drilling tools made of these materials and higher drilling rates.

## 9.5 Summary

MPC is a technique based on the quasi-dynamic pressing of powders. It does not employ strain rates of the level usual for the dynamic compaction; however, its deformation rates by orders of magnitude exceed those in the conventional quasi-static powder pressing. It should be also noted that MPC does not usually involve any direct interaction of the magnetic field with powder materials. Rather, it uses the kinetic energy of the tooling rendering the conditions of the quasi-dynamic compaction. This intermediate position of MPC between quasi-static and dynamic compaction of powders provides it with some rather unique capabilities, including the preservation of the nanostructure of the obtained materials and the suitability for a wide range of shapes – from disks and tablets to rods and tubes of great length. Unlike dynamic pressing, MPC generates an acclivous leading edge of the compression wave, which excludes the emergence of the next discharge wave and avoids exfoliation of the compacts. The method is divided into uniaxial pressing and radial pressing. The understanding of the processes taking place during MPC has been advanced in the last decade thanks to computer modeling. The following are promising directions for the development of MPC technology: the use of multiple pulses, repeated pressing of tablets with overturning, expansion of the shell at the end of the pulse, and the combination of MPC with SPS.

## References

1. Mironov VA (1980) Magnetic pulsed pressing of powders. Zinatie, Riga, USSR, 196 p, (in Russian)
2. Sandstrom DJ (1964) Consolidating metal powders magnetically. *Met Prog* 8:215–221
3. Barbarovich YK (1969) Use of the energy of a strong pulsed magnetic field for powder compaction. *Soviet Powder Metall Metal Ceram* 8(10):798–803
4. Knopfel G (1972) Superstrong magnetic fields. *Mir*, Moscow, 383 p, (in Russian)
5. Ivanov VV, Pararin SN, Vikhrev AN, Nozdrin AA (1997) *Materialovedenie (Materials Science)* 5:49 (in Russian)
6. Ivanov VV, Vikhrev AN (1997) *Fizika I Khimiya Obrabotki Materialov. Phys Chem Mater Process* 3:67 (in Russian)
7. Pararin S, Ivanov V, Nikonov A, Spirin A, Khrustov V, Ivin S, Kaygorodov A, Korolev P (2006) Densification of nano-sized alumina powders under radial magnetic pulsed compaction. *Adv Sci Technol* 45:899–904
8. Ivanov VV, Ivin SY, Khrustov VR, Kotov YA, Murzakaev AM, Nikonov AV, Pararin SN, Spirin AV (2005) Fabrication of nanoceramic thin-wall tubes by magnetic pulsed compaction and thermal sintering. *Sci Sinter* 37:55–60

9. Boltachev GS, Nagayev KA, Pararin SN, Spirin AV, Volkov NB (2010) Magnetic pulsed compaction of nanosized powders. Nova Science Publishers, New York
10. Boltachev GS, Volkov NB, Kaygorodov AS, Loznukho VP (2011) The peculiarities of uniaxial quasistatic compaction of oxide nanopowders. *Nanotechnologies Russia* 6(9–10):639–646
11. Park HY, Fatih Kilicaslan M, Hong SJ (2012) Effect of multiple pressures by magnetic pulsed compaction (MPC) on the density of gas-atomized Al-20Si powder. *Powder Technol* 224:360–364
12. Li M, Yu H, Li C (2010) Microstructure and mechanical properties of Ti6Al4V powder compacts prepared by magnetic pulse compaction. *Trans Nonferrous Met Soc China* 20:553–558
13. Dobrov SV, Ivanov VV (2004) Simulation of pulsed magnetic molding of long powdered products. *Tech Phys* 49:413–419
14. Boltachev GS, Volkov NB, Ivanov VV, Kaygorodov AS (2009) Shock-wave compaction of the granular medium initiated by magnetically pulsed accelerated striker. *Acta Mech* 204:37–50
15. Boltachev GS, Kaygorodov AS, Volkov NB (2009) Densification of the granular medium by the low amplitude shock waves. *Acta Mech* 207:223–234
16. Boltachev GS, Nagayev KA, Pararin SN, Spirin AV, Volkov NB (2010) Theory of the magnetic pulsed compaction of nanosized powders. In: Cabral V, Silva R (eds) *Nanomaterials: properties, preparation and processes*. Nova Science Publishers, New York, pp 1–58
17. Boltachev GS, Volkov NB, Dobrov SV, Ivanov VV, Nozdrin AA, Pararin SN (2007) Simulation of radial pulsed magnetic compaction of a granulated medium in a quasi-static approximation. *Tech Phys* 52(10):1306–1315
18. Boltachev GS, Volkov NB, Pararin SN, Spirin AV (2010) Dynamics of cylindrical conducting shells in a pulsed longitudinal magnetic field. *Tech Phys* 55:753–761
19. Boltachev GS, Volkov NB (2009) Expansion of a conducting shell by magnetic field of an external inductor. *Tech Phys Lett* 35:334–336
20. Boltachev GS, Volkov NB (2009) Bimetallic cylinder in a pulsed magnetic field. *Tech Phys Lett* 35:916–919
21. Olevsky EA, Bokov AA, Boltachev GS, Volkov NB, Zayats SZ, Ilyina AM, Nozdrin AA, Pararin SN (2013) Modeling and optimization of uniaxial magnetic pulse compaction of nanopowders. *Acta Mech* 224(12):3177–3195
22. Shtern MB, Serdyuk GG, Maksimenko LA, Truhan YV, Shulyakov YM (1982) Phenomenological theories of powder pressing. *Naukova Dumka, Kiev* (in Russian)
23. Olevsky E (1998) Theory of sintering: from discrete to continuum. *Mater Sci Eng R* 23:41–100
24. Olevsky EA, Molinari A (2000) Instability of sintering of porous bodies. *Int J Plast* 16:1–37
25. Olevsky EA, Molinari A (2006) Kinetics and stability in compressive and tensile loading of porous bodies. *Mech Mater* 38:340–366
26. Olevsky EA, LaSalvia JC, Ma J, Meyers MA (2007) Densification of porous bodies in a granular pressure-transmitting medium. *Acta Mater* 55:1351–1366
27. Shtern M, Olevsky E (2008) Plastic behavior of agglomerated powder. *Comput Mater Sci* 43:704–709
28. Ivashutenko AS (2010) Alumina-zirconia nanoceramics obtained with the use of high energy flows. PhD Dissertation, Tomsk Polytechnic University, Tomsk (in Russian)
29. Yu HP, Li CF (2007) Dynamic compaction of pure copper powder using pulsed magnetic force. *Acta Metall Sin (English Letters)* 20(4):277–283
30. Andrievskii RA, Vikhrev AN, Ivanov VV, Kuznetsov RI, Noskova NI, Sazonova VA (1996) Magnetic-pulse and high-pressure shear-strain compaction of nanocrystalline titanium nitride. *Fiz Metall Metalloved* 81:137–145 (in Russian)
31. Ivanov VV, Kotov YA, Samatov OH, Böhme R, Karow HU, Schumacher G (1995) Synthesis and dynamic compaction of ceramic nano powders by techniques based on electric pulsed power. *Nanostruct Mater* 6(1–4):287–290
32. Nozdrin AA (2007) Investigation of the possibilities of dynamic pressing of alumina-based nanopowders. *Perspektivnye Materialy* 6:79 (in Russian)

33. Boltachev GS, Volkov NB (2010) Size effect in compaction of nanopowders. *Pis'ma v Zhurnal Technicheskoi Fiziki* (Technical Physics Letters) 36(17):96 (in Russian)
34. Boltachev GS, Volkov NB (2011) Simulation of nanopowder compaction in terms of granular dynamics. *Tech Phys* 56(7):919–930
35. Kaygorodov AS, Ivanov VV, Paranin SN, Nozdrin AA (2007) The role of adsorbed species on pulse pressing of oxides. *Rossiiskie Nanotekhnologii* 2(1–2):112–118 (in Russian)
36. Guzeyev VV (1995) Temperature control of zirconia ceramics sintering. *Glas Ceram* 10:25–29 (in Russian)
37. Chelluri B, Knoth E (2010) 4th international conference on high speed forming. Columbus
38. Lee GH, Rhee CK, Lee MK, Kim WW, Ivanov VV (2004) Nanostructures and mechanical properties of copper compacts prepared by magnetic pulsed compaction method. *Mater Sci Eng A* 375–377(15):604–608
39. Rhee CK, Lee GH, Kim WW, Ahn JH, Hahn YD (2003) Correlation between structure and mechanical properties for nano-crystalline copper prepared by pulsed compaction. *J Metastable Nanocryst Mater* 15–16:757–763
40. Lee GH, Rhee CK, Kim KH (2003) The effect of compaction temperature and pressure on the pores in nanostructured metal compacts prepared by magnetic pulsed compaction. *Metals Mater Int* 9(4):375–378
41. Han YS, Seong BS, Lee CH (2004) SANS study of microstructural inhomogeneities on Al nano-powder compacts. *Physica B Cond Matter* 350(1–3):E1015–E1018
42. Hong SJ, Lee GH, Rhee CK (2007) Magnetic pulsed compaction of ferromagnetic nanopowders for soft-magnetic core. *Mater Sci Eng A* 449–451(25):401–406
43. Chelluri B (1994) Dynamic magnetic consolidation (DMC) process for powder consolidation of advanced materials. *Mater Manuf Proc* 9(6):1127–1142
44. Chae HJ, Kim YD, Kim TS (2011) Microstructure and mechanical properties of rapidly solidified Mg alloy powders compacted by magnetic pulsed compaction (MPC) method. *J Alloys Compd* 509(1):S250–S253
45. Banin VE, Boehme R, Schumacher G, Vikhrev A (1995) Dynamic compaction of nanosized ceramic oxide powders. *Mater Sci Forum* 225–227:623–628
46. Ivanov VV, Khurstov VR (1998) *Inorg Mater* 34(4):39–43 (in Russian)
47. Kaygorodov A, Rhee C, Kim W, Ivanov V, Paranin S, Spirin A, Khurstov V (2007) Nozzles from alumina ceramics with submicron structure fabricated by radial pulsed compaction. *Mater Sci Forum* 534–536:1053–1056
48. Hong SJ, Lee JK, Lee MK, Sung JH, Lee CG, You YZ (2006) Consolidation of Al<sub>2</sub>O<sub>3</sub> nanopowder by magnetic pulsed compaction and sintering. *Solid State Phenom* 118:615–622
49. Hong SJ, Koo JM, Lee JG (2009) Precompaction effects on density and mechanical properties of Al<sub>2</sub>O<sub>3</sub> nanopowder compacts fabricated by magnetic pulsed compaction. *Mater Trans* 50(12):2885–2890
50. Lee J, Hong SJ, Lee MK, Sung JH, Lee CG, You YZ (2006) Fabrication of high-density nanostructured alumina by the combined processes of magnetic pulsed compaction (MPC) and Spark Plasma Sintering (SPS). *Solid State Phenom* 118:597–602
51. Dyatlova YG, Romyantsev VI, Ordan'yan SS, Osmakov AS, Zayats SV, Ivanov VV, Paranin SN (2013) Website of “Virial”, Ltd. (electronic source, free access): [http://www.virial.ru/upload/medialibrary/85a/Tezisy\\_2.pdf](http://www.virial.ru/upload/medialibrary/85a/Tezisy_2.pdf). (in Russian)
52. Ivanov VV, Paranin SN, Khurstov VR (2002) Nanostructured ceramics based on aluminum and zirconium oxides produced using magnetic pulsed pressing. *Phys Metals Metallogr* 94(1):S98–S106
53. Banin VE, Paranin S, Khurstov V, Medvedev A, Shtol'ts A (2002) Processing of nanostructured oxide ceramics with magnetic pulsed compaction technique. *Key Eng Mater* 206–213:377–380
54. Lee JG, Hong SJ, Park JJ (2010) Fabrication of an yttria thin-wall tube by radial magnetic pulsed compaction of powder-based tapes. *Mater Trans* 51(9):1689–1693
55. Lee JK, Hong SJ, Lee MK, Rhee CK (2007) Fabrication of high density Y<sub>2</sub>O<sub>3</sub> ceramics by magnetic pulsed compaction. *Solid State Phenom* 119:175–178

56. Ivanov VV, Kaigorodov AS, Khrustov VR, Paragin SN, Spirin AV (2006) High-strength alumina-based ceramics produced by magnetic pulsed compaction of composite nanopowders. *Rossiiskie Nanotehnologii* 1(1–2):201–207 (in Russian)
57. Lee JG, Lee MK, Hong SJ, Lee HW, Pyun SP, Rhee CK (2010) Consolidation of mixed diamond and cobalt granule powders by magnetic pulsed compaction. *Mater Lett* 64(1):35–37